Spatiotemporal patterns of γ frequency oscillations tetanically induced in the rat hippocampal slice

Miles A. Whittington, Ian M. Stanford *, Simon B. Colling *, John G. R. Jefferys * and Roger D. Traub †‡§

*Department of Physiology and Biophysics, Imperial College School of Medicine at St Mary's, Norfolk Place, London W2 1PG, UK, *Department of Physiology, The Medical School, University of Birmingham, Birmingham B15 2TT, UK, †IBM Research Division, T. J. Watson Research Center, Yorktown Heights, NY 10598, USA and ‡Department of Neurology, Columbia University, New York, NY 10032, USA*

1. We used transverse and longitudinal rat hippocampal slices to study the synchronization of γ frequency (> 20 Hz) oscillations, across distances of up to 4·5 mm. γ oscillations were evoked in the CA1 region by tetanic stimulation at one or two sites simultaneously, and were associated with population spikes. Tetanic stimuli that were strong enough to induce oscillations were associated with depolarization of both pyramidal cells and interneurones, largely produced by activation of metabotropic glutamate receptors.

2. Computer simulations of γ oscillations were also performed in a model with pyramidal cells and interneurones, arranged in a chain of five cell groups. This model had suggested previously that interneurone networks alone could generate synchronous γ oscillations locally, but that pyramidal cell firing, by inducing spike doublets in interneurones, was necessary for the occurrence of highly correlated oscillations with small phase lag (< 2·5 ms), in a distributed network possessing long axon conduction delays.

3. In both experiment and model, pyramidal cell spikes occurred in phase with local population spikes, as did the first spike of the interneurone doublet.

4. The conductance of the interneurone α-amino-3-hydroxy-5-methyl-4-isoxazole propionic acid (AMPA) receptor-mediated conductance was manipulated in the model, while the relation between oscillations at opposite ends of the chain was examined. When the conductance was large enough for doublet firing to be synaptically induced in interneurones, oscillation phase lags were < 2·25 ms across the chain. As predicted, experimental blockade of AMPA receptors resulted in increased phase lags between two sites oscillating simultaneously, compared with control conditions.

5. Both in model and in experiment, when stimuli to the two ends of the network were slightly different, cross-network synchronization occurred with a shorter phase lag at high frequencies than at lower frequencies.

6. These data suggest that, while interneurone networks alone can generate locally synchronized γ oscillations, firing of pyramidal cells, and the synaptically induced doublet firing in interneurones, contribute to the stability and tight synchrony of the oscillations in distributed networks.

γ frequency (used here to mean > 20 Hz) oscillations are found in hippocampal and thalamocortical systems during wakefulness and ketamine–xylazine anaesthesia, as well as during slow-wave sleep (Bragin, Jandó, Nádasdy, Hetke, Wise & Buzsáki, 1995; Singer & Gray, 1995; Steriade, Amzica & Contreras, 1996*a*). During wakefulness and anaesthesia, γ oscillations can be widely distributed (≥ 7 mm) with phase lags of a few milliseconds or less (Engel, Kreiter, König & Singer, 1991; Frien, Eckhorn, Bauer, Woelbern & Kehr, 1994), and the γ oscillations appear to have behavioural significance in that they occur during complex motor acts (Murthy & Fetz, 1992), or after

§ To whom correspondence should be addressed at the Department of Physiology, The Medical School, University of Birmingham, Vincent Drive, Birmingham B15 2TT, UK.

specific sensory stimulation. In the latter case, synchronization of oscillations over long distances tends to occur when brain regions are simultaneously activated by features of a common object (Gray, König, Engel & Singer, 1989), with neurones stimulated less than optimally by this object oscillating at the same frequency but with phase lags (of a few milliseconds) with respect to the mean (König, Engel, Roelfsema & Singer, 1995). It seems possible that γ oscillations could therefore be of functional importance, both for information processing during the oscillation, and perhaps also for establishing memory traces of perceptual events. This motivates efforts to understand the cellular mechanisms of γ oscillations.

While information-processing questions to do with γ oscillations have related principally to the neocortex and olfactory cortex, the rat CA1 region *in vitro* has provided a useful experimental system. γ frequency oscillations can be readily evoked in CA1 by tetanic stimulation or by application of metabotropic glutamate receptor agonists (Whittington, Traub & Jefferys, 1995), as well as by muscarinic agonists (Borroni & Levy, 1996). With tetanic stimulation at two or more sites, oscillations in CA1 can become tightly synchronized (< 1 ms mean phase lag) at distances of at least 4·5 mm (Traub, Whittington, Stanford & Jefferys, 1996*b*; I. M. Stanford & J. G. R. Jefferys, unpublished data), so that an important feature of the *in vivo* phenomenon is captured *in vitro*. The relative sparseness of pyramidal cell–pyramidal cell synaptic connections in CA1 *in vitro* (Knowles & Schwartzkroin, 1981; Christian & Dudek, 1988; Thomson & Radpour, 1991) renders the analysis of the circuitry simpler than is the case in the neocortex.

Electrophysiological data from the CA1 region *in vitro*, along with network simulations of compartmental neurones, suggest that synaptically interconnected networks of interneurones alone can generate γ oscillations, but that the properties of the oscillation are modified, in important ways, by the participation of pyramidal cells. Networks of interneurones (i-cells), without pyramidal cells (e-cells), can generate γ oscillations, at least locally, when the interneurones are depolarized enough to fire spontaneously. The frequency of this oscillation is determined by the interneuronal depolarization, as well as by the properties of the interneurone–interneurone $GABA_A$ receptor-mediated synaptic connections, particularly the synaptic conductance amplitude and relaxation time constant (Whittington *et al.* 1995; Traub, Whittington, Colling, Buzsáki & Jefferys, 1996*a*).

Pyramidal cells can participate in the oscillation as well, when they too are sufficiently depolarized (see below). Simulations predict that nearby pyramidal cells and interneurones should oscillate in phase (lag < 1 ms) (Traub *et al.* 1996*b*). If the AMPA (α-amino-3-hydroxy-5-methyl-4-isoxazole propionic acid) receptor-mediated conductance at pyramidal cell–interneurone connections is large enough, then presynaptic pyramidal cell firing causes the interneurones to fire spike doublets, action potential pairs at intervals of less than about 8 ms. In simulations, doublet firing allows distributed networks of neurones to produce γ oscillations that are tightly phase-locked (lags less than about 2 ms) across the array, despite axon conduction delays of over 10 ms (Traub *et al.* 1996*b*). Such conduction delays are likely in distributed networks in the brain, as pyramidal cell and interneurone local axon conduction velocities are slow: about 0·5 m s^{-1} for CA1 pyramidal cell axons (S. B. Colling & J. G. R. Jefferys, unpublished data), 0·15–0·55 m s^{-1} for neocortical pyramidal cells (Murakoshi, Guo & Ichinose, 1993), and 0·06–0·20 m s^{-1} for neocortical interneurone collaterals (Salin & Prince, 1996). A 0·2 m s^{-1} (0·2 mm ms^{-1}) velocity produces a delay of 20 ms at 4 mm. Experimentally, most CA1 stratum pyramidale interneurones so far recorded (6 out of 8) do fire doublets, at least part of the time, when synchronized γ oscillations are evoked over spatial scales of 2 mm or more, whereas interneurones fire only single action potentials when oscillations are evoked locally.

Here, we examined certain parameters that regulate the extent of oscillatory synchronization and of phase lags, in a distributed network: the amplitude of the pyramidal cell–interneurone AMPA receptor-mediated conductance (which determines the extent of interneurone doublet firing), and the uniformity or non-uniformity of simultaneous stimuli that evoke oscillations at distinct – but coupled – sites. As before, we used a combined experimental–simulation approach. Three predictions of the network model are confirmed experimentally: on the phase relation of pyramidal cell *vs.* interneurone firing, on the frequency dependence of phase differences across a distributed network, and on the effects on phase relations of AMPA receptor blockade. The data suggest that interneurone doublet firing helps to keep the oscillation synchronized over distance, and that interneurone doublet firing tends to maintain synchrony when stimulation of the system is not uniform spatially.

METHODS

Experimental methods

Transverse dorsal and longitudinal CA1 hippocampal slices, 400–450 μm thick, were prepared from brains of forty-seven male Sprague–Dawley rats (200–300 g), which were either stunned or anaesthetized by an intraperitoneal injection of Domitor (medetomidine hydrochloride, 1 mg ml^{-1}; SmithKline Beecham) and Vetalar (ketamine hydrochloride, 100 mg ml^{-1}; Parke-Davis Veterinary, Cambridge, UK), then killed by cervical dislocation followed by decapitation. Slices were maintained at 33–35 °C at the interface between warm, wetted 95% O_2–5% CO_2 and artificial cerebrospinal fluid (ACSF) containing (mM): NaCl, 135; KCl, 3 or 4; $NaHCO_3$, 16; NaH_2PO_4, 1·25; $CaCl_2$, 1·5–2; $MgCl_2$, 0·8–1·0; D-glucose, 10.

γ oscillations were evoked by simultaneous tetanic stimulations (15–20 pulses; width, 50 μs; 6–90 V; at 80–100 Hz) delivered by bipolar stimulating electrodes placed in either stratum oriens, stratum radiatum or stratum pyramidale, near to two recording sites: one at the subicular end, and the other at the CA2 end of the CA1 region. The distance between stimulation sites was dictated by

Table 1. Parameters of physiologically identified neurones

Putative cell type	AP (ms)	fAHP amplitude (mV)	fAHP duration (ms)	Maximum frequency (0–99 ms) (Hz)	Frequency (100–199 ms) (Hz)	Frequency (200–299 ms) (Hz)	V_m (mV)	R_{input} (MΩ)
i-cell ($n = 8$, $*n = 5$)	0·6 ± 0·1	9·8 ± 1·0	21·4 ± 1·6	333 ± 23*	248 ± 11*	220 ± 7*	−62 ± 3	38 ± 4
e-cell ($n = 10$)	1·1 ± 0·1	4·2 ± 0·6	—	118 ± 10	24 ± 4	11 ± 4	−69 ± 4	42 ± 5

AP, action potential width at half-amplitude; fAHP, fast after-hyperpolarization, measured from baseline pre-spike to initial peak negativity for amplitude, and to return to baseline for duration (in i-cells); V_m, membrane potential; R_{input}, input resistance. i-cell action potentials used for AHP measurements were spontaneous, and e-cell action potentials used for AHPs were in response to minimal depolarizing current injection. fAHP duration could not be determined in e-cells, because it merged into a long-lasting AHP. Frequencies are in response to intracellular current injection of 0·6 nA. Values are means ± S.E.M.

the length of the CA1 region in each slice, and ranged from 1·2 to 4·5 mm measured along stratum pyramidale. Tetanic stimuli were matched between the two sites using the amplitude of an antidromically elicited population spike generated in response to a single stimulus pulse. Oscillations generated by tetanic stimulation of stratum oriens tended to be more localized spatially than oscillations generated by stratum radiatum stimulation.

Extracellular recordings of field oscillations were taken at both sites using glass micropipettes filled with 2 or 3 M NaCl (resistance, 1–5 MΩ) placed in the stratum pyramidale. Intracellular recordings of somatic potentials were taken using glass micropipettes filled with 2 M potassium acetate or potassium methylsulphate (resistance, 30–75 MΩ). Cells were selected for use in the study by the following criteria: membrane potential more negative than −55 mV, input resistance greater than 30 MΩ, action potential peak greater than +5 mV. Cells were designated e-cells (pyramidal cells) or i-cells (stratum pyramidale interneurones) on the basis of the action potential morphology and response to depolarizing current injection (1 s, 0·3 and 0·6 nA). Approximately one in fifty impaled cells displayed the properties of a fast-spiking (> 300 Hz), partially accommodating interneurone. Parameters of putative i-cells (interneurones) and e-cells (pyramidal cells) are summarized in Table 1. Both intra- and extracellular recording sites were kept as close to the stimulation site as possible at either end of CA1, to allow low stimulus intensities to be used and thus keep the activation of CA1 local. Recordings were digitized and analysed using a CED analogue/digital converter and associated software (Cambridge Electronic Design, Cambridge, UK).

Experiments examining the effects of blockade of fast glutamatergic neurotransmission were carried out using pressure ejection (1·75–2·10 kg cm^{-2} (25–30 psi), 4 ms pulse width) of NBQX (6-nitro-7-sulphamoylbenzo(*f*)quinoxaline-2,3-dione; 1–100 μM in ACSF). Ejection pipettes were fashioned from extracellular microelectrodes with tips broken back to give resistances of 100–500 kΩ when filled with 2 M NaCl. NBQX was ejected onto the slice between the two recording sites, proximal to the subicular site, distal to the CA2 site. NBQX (20 μM) was also added to the bath solution in some experiments.

The origins of the tetanically induced depolarization were investigated in pyramidal cells using bath application of the following drugs: D-2-amino-5-phosphopentanoic acid (D-AP5; 50 μM) to block the *N*-methyl-D-aspartate (NMDA) subtype of glutamate receptor; (*S*)-α-4-carboxyphenylglycine (MCPG; 0·2 mM) to block non-specifically metabotropic glutamate receptors; and 1,1-dimethyl-4-diphenylacetoxypiperidinium iodide (4-DAMP; 1 μM) and 2-diethylaminoethyl-1-(4-nitrophenyl) cyclopentanecarboxylate (Nitrocaramiphen; 1 μM) to block muscarinic cholinergic receptors (M_3 and M_1 subtypes, respectively).

The extracellular potassium concentration was measured, 100–200 μm from the stimulation site, using single-barrelled K^+-sensitive electrodes (Heinemann, Lux & Gutnick, 1977). Briefly, silanized, thick-walled glass micropipettes (1–2 MΩ) were filled with 100 mM NaCl and 5 mM KCl. The tip was then filled with the potassium ionophore I cocktail B (Fluka, Buchs, Switzerland), giving a final resistance of 1–10 GΩ. The electrodes were calibrated by measuring the voltage change corresponding to 3, 5 and 10 mM extracellular K^+.

Simulation methods

The structure of the network model was the same as in Traub *et al.* (1996*b*), with the exception that we now did not use any slow synaptic currents: the NMDA conductance in recurrent pyramidal→interneurone connections was omitted, and instead both pyramidal cells and interneurones were driven by steady depolarizing currents. (The reason for this omission was that experiments showed relatively little effect of NMDA blockers on the tetanically induced oscillations; Fig. 1.) Briefly, the model network consisted of five subnetworks, each with eight pyramidal cells (e-cells) and eight interneurones (i-cells, representing basket cells). The five subnetworks were arranged into a chain of 'cell groups' numbered 1 to 5. Synaptic connections are formed between cells within subnetworks, and between cells in neighbouring subnetworks, but not between cells in distant subnetworks. Axon conduction delays exist for connections between neighbouring cell groups, but are insignificant for connections within a group. The network model did not include any gap junctions, and we did not simulate extracellular field (ephaptic) effects.

The forty pyramidal cells in the model are too few to simulate a continuum of cells, something more appropriate to the thousands of pyramidal cells in CA1 *in vitro*. Instead, we think of the chain of cell groups as representing selected subsets of cells, separated by a distance of 500–600 μm. In that way, the total length of the chain is about 2·0–2·4 mm, i.e. most of the length along stratum

pyramidale of CA1 in a transverse slice. The distance 500–600 μm corresponds to the average spread in one direction of a basket cell axon (Sik, Penttonen, Ylinen & Buzsáki, 1995). *In vivo*, the spread of CA1 pyramidal cell axons, within CA1, can be up to 1·5 mm caudally and up to about 0·5 mm rostrally (Tamamaki & Nojyo, 1990). Depending on how a slice is cut, the 500–600 μm intergroup separation may be either about right, or too small, for the CA1 pyramidal cell axon spread. On the other hand, CA1 pyramidal cell collaterals are expected to innervate cells in target fields with lower probability than do basket cells (Knowles & Schwartzkroin, 1981; Sik *et al.* 1995), so that the effect of longer-range CA1 pyramidal axons may not be critical.

Of course, basket cells and pyramidal cells do not exist in a 1 : 1 ratio in the hippocampus, interneurones of all types constituting a minority of the cells. As will be seen below, however, virtually all CA1 pyramidal cells fired continuously during the tetanically induced γ oscillations to be described, as did virtually all stratum pyramidale interneurones. The cells in the network model then correspond to some arbitrary subset of the real population of neurones. This representation would be harder to justify if only some of the neurones were firing.

Intrinsic cell properties

Pyramidal cells were simulated using a multicompartment model of a CA3 pyramidal neurone (Traub, Jefferys, Miles, Whittington & Tóth, 1994). CA3 cells, when injected with sufficiently large depolarizing currents, fire repetitive single action potentials rather than intrinsic bursts (Wong & Prince, 1981), as do most CA1 cells during injection of depolarizing current (Schwartzkroin, 1978) and after tetanic stimulation in our experiments (see below). Therefore, the model pyramidal cell appears to be adequate for the purpose at hand. Interneurones were simulated with the multicompartment model of Traub & Miles (1995). Doublet firings do not occur in this model during injection of depolarizing current into single isolated interneurones, as was true experimentally (Fig. 1).

Network topology

Each cell (e-cell or i-cell) received input from sixteen e-cells and sixteen i-cells. Eight of these presynaptic e-cells (respectively i-cells) are the cells of the postsynaptic cell's own group (hence autapses are allowed), while the remaining eight presynaptic cells are from neighbouring groups. If the postsynaptic cell is in an end group (group 1 or group 5), then there is only one neighbouring group (group 2 or group 4); each cell in the end group receives input from all of the cells in the neighbouring group. If the postsynaptic cell is in a middle group (groups 2, 3 and 4), then there are two neighbouring groups: four cells from the left, and four cells from the right are then presynaptic.

Details of synaptic actions

$GABA_A$ receptor-mediated conductances have instantaneous onset and decay with time constants of 10 ms. The total peak conductance of a unitary IPSC is 4·0 nS on a pyramidal cell, and 1·5 nS on an interneurone. Each presynaptic interneurone forms contacts on the soma and most proximal dendritic compartments of postsynaptic pyramidal cells (Buhl, Cobb, Halasy & Somogyi, 1995), with conductance in each compartment in proportion to its surface area. Interneurone→interneurone synaptic contacts are each to a single compartment, any of seven in the proximal dendrites. IPSCs onto a given compartment from different presynaptic cells, or from the same cell at different times, are added together, subject to the constraint (on i-cells) that no one compartment ever develops a conductance of more than 12·0 nS (i.e. there is conductance saturation).

Unitary AMPA receptor-mediated conductances have a time course: $c_{e\rightarrow i} t e^{-t}$, where $c_{e\rightarrow i}$ is a scaling constant, from 0·0 to 8·0 nS, and t is time in milliseconds. This unitary conductance will have a peak value of $c_{e\rightarrow i}/e$, where $e = 2{\cdot}718...$ When $c_{e\rightarrow i}$ is 8·0 nS, single presynaptic action potentials can evoke a postsynaptic action potential; note, however, that during a synchronized population oscillation, each interneurone will receive multiple nearly simultaneous EPSCs from many presynaptic neurones. Excitatory connections are made onto single interneurone compartments, chosen from any of eighteen different compartments in the middle dendrites. As for IPSCs, EPSCs from different presynaptic e-cells, and at distinct times, are added together, subject to saturation: no compartment can develop an excitatory conductance greater than 5 nS.

Recurrent pyramidal–pyramidal synaptic connections do exist in CA1 *in vitro*, but apparently with low density (Knowles & Schwartzkroin, 1981; Christian & Dudek, 1988; Thomson & Radpour, 1991). Such interactions were omitted in the present simulations.

Driving currents to the neurones

Tetanic stimulation of the slice leads to intracellular depolarizations (see below). To produce a similar effect, we excited the model neurones with depolarizing somatic currents, of the form I + offset, where I is a constant for each cell type and each simulation (in nanoamps), and the offset introduces small differences in driving currents between different cells. For i-cells, the offset is (0·01/40 × cell-number), where the cell number is 1, 2...40. For e-cells, the offset is (0·01/40 × cell-number) + (0·2/8 × cell-number-within-group), the cell-number-within-group being 1, 2...8. Metabotropic glutamate receptor activation of the neurones is expected to be associated with a conductance change and a reversal potential near 0 mV, rather than simply a current injection, (Pozzo Miller, Petrozzino & Connor, 1995), but this does not produce significant changes in the results. In control simulations, we found network oscillations with similar appearance to those reported here, when pyramidal cells and interneurones were driven by tonic excitatory conductances, having a reversal potential 60 mV positive to resting potential.

Axon conduction delays

Model pyramidal cells and interneurones each contain short axonal segments, of five compartments each, that lead to delays of less than 0·5 ms from the peak of the somatic action potential to the peak of the action potential in the most distal axonal compartment. This short delay will be referred to as d. The axon conduction delay between cells within the same cell group is simply d itself. The axon conduction delay between neighbouring cell groups is d + 4 ms. If we imagine the distance between neighbouring cell groups to be 550 μm, and ignore d, this corresponds to a conduction velocity of 0·14 m s^{-1}, a value within the range observed for inhibitory cell collaterals in neocortex (Salin & Prince, 1996), at the low end of the range for neocortical pyramidal cell collaterals (Murakoshi *et al.* 1993), and below the 0·5 m s^{-1} measured for CA1 pyramidal cell principal axons (S. B. Colling & J. G. R. Jefferys, unpublished data). Local collaterals of CA1 pyramidal cell axons would, however, be expected to conduct more slowly than the principal axon.

Noise in the system

Random noise was present in the network in the form of ectopic axonal action potentials, generated by small current pulses in distal axons induced with Poisson statistics. The mean frequency was 1 per 5 s for each pyramidal cell axon, and 1 s^{-1} for inhibitory cell axons.

Data analysis

Simulations were run for 1500 ms. Data saved included somatic potentials of sixteen pyramidal cells and sixteen interneurones, four cells of each type from each of four groups: every group but the middle one. Autocorrelations were performed on the last 750 ms of each run, using an average of four cell voltages in group 1 and in group 5; cross-correlations were performed with the same data. Cross-correlation amplitudes were measured from the peak (nearest to 0) to the nearest trough at positive times; these amplitudes were then normalized with respect to the biggest amplitude in a pool of simulations.

Computing details

Simulations were run using eight nodes of an IBM SP1 or SP2 parallel computer, with the differential equations for five e-cells and five i-cells integrated on each node. A simulation of 1500 ms took about 1·8 h on an SP2. Computer simulations were performed at the IBM T. J. Watson Research Center, while slice experiments were performed at Imperial College School of Medicine at St Mary's and at the University of Birmingham.

Results are given as means ± S.E.M.

RESULTS

Intracellular correlates of tetanically induced oscillations

Tetanic stimuli sufficient to induce population oscillations had predictable effects on the membrane potential of pyramidal cells and of interneurones (Fig. 1). In each case a slow depolarization was produced, lasting 0·5–2 s, with a magnitude of 23 ± 2 mV for e-cells (resting membrane potential, −69 ± 4 mV; $n = 10$ cells), and 17 ± 2 mV for i-cells (resting membrane potential, −62 ± 3 mV; $n = 8$ cells). There was always a latent period between the end of the tetanic stimulus and the onset of action potentials. This latent period was 121 ± 18 ms for e-cells and 132 ± 22 ms for i-cells. In e-cells, the spike after-hyperpolarization became undetectable during the slow depolarization.

The firing properties of interneurones and of pyramidal cells were different, depending on whether the cell was stimulated by intracellular current injection, or whether the cell was participating in a tetanically evoked oscillation (Fig. 1*B*). Physiologically identified interneurones (i-cells) fired, in response to depolarizing current injection, with rhythmic action potentials at frequencies up to 400 Hz. During high-frequency repetitive firing induced by current stimuli in interneurones, doublet firing was not observed (Fig. 1*B*). Such a pattern of rhythmic firing has been reported for basket cells *in vivo* (Sik *et al.* 1995) and *in vitro* (Buhl *et al.* 1995), and for oriens/alveus interneurones *in vitro* (Lacaille, Mueller, Kunkel & Schwartzkroin, 1987). Axo-axonic cells *in vitro* can, however, fire doublets in response to current injection, apparently as an intrinsic property (Buhl, Han, Lörinczi, Stezhka, Karnup & Somogyi, 1994).

Physiologically identified pyramidal cells (e-cells) fired, in response to a depolarizing current injection, adapting trains of action potentials, with considerably longer interspike intervals than i-cells and at no stable fixed frequency. Action potential widths were 4–6 ms for e-cells and 2–3 ms for i-cells.

During the tetanically induced oscillation, in contrast, both cell types fired rhythmically at γ frequencies. As reported previously (Traub *et al.* 1996*b*), during two-site oscillations – but not during single-site oscillations – many of the interneurones fired spike doublets, although not necessarily after each paired tetanus or during each wave. Six out of eight interneurones that met recording criteria (see Methods) fired either occasional doublets or trains of doublets after two-site stimulation. Specifically, each of these six interneurones fired doublets during more than 50% of oscillatory trains. In the course of fifteen dual-site-stimulated oscillatory trains (in these 6 interneurones), during periods of either synchrony or fixed phase lag between the two sites, a total of thirty-seven doublets occurred over 122 oscillatory waves, i.e. doublets occurred on 30% of the waves. When spike doublets did not occur, the interneurone action potential was followed by an EPSP with an amplitude of 4·2 ± 0·6 mV in 69% of cases (59/85 instances; baseline potential, −59 to −51 mV); some of these EPSPs could induce spike doublets in the axon, in principle. The mean intradoublet spike interval was 5·2 ± 0·2 ms ($n = 37$ doublets).

The origin of the tetanically induced depolarization in pyramidal cells was examined by application of drugs (Fig. 1*C*). Blockade of NMDA receptors with D-AP5 (50 μM) reduced the duration of the depolarization without marked effect on peak amplitude, and the duration could be returned to its preblockade value by increasing the stimulus strength 2-fold. Additional application of the non-specific metabotropic glutamate receptor blocker MCPG (0·2 mM) left only a small brief depolarization, without action potentials. In contrast, the M_3 muscarinic receptor antagonist 4-DAMP (1 μM) had little effect on the depolarization induced in CA1 pyramidal cells by tetanic stimulation. Co-application of an M_1 muscarinic receptor antagonist (Nitrocaramiphen; 1 μM) reduced the duration of the depolarization (to 50% at half-width) and also reduced the duration of the oscillation. Again, MCPG abolished the oscillation completely and left only a small brief depolarization. These data suggest that the tetanically induced depolarization results mainly from activation of metabotropic glutamate receptors, but that M_1 muscarinic receptors do make some contribution.

Extracellular potassium

Following tetanic stimulation (50–70 V), $[K^+]_o$ could reach 8·2 ± 1·5 mM ($n = 6$ measurements), 200 μm from the stimulation site (data not shown). Peak values of $[K^+]_o$ were attained at 1·27 ± 0·13 s after the stimulus. Nevertheless, such high values of $[K^+]_o$ were not *essential* for the oscillation to occur: in two cases (Fig. 2), oscillations were induced wherein $[K^+]_o$ rose only to 4·1 and 5·5 mM, respectively.

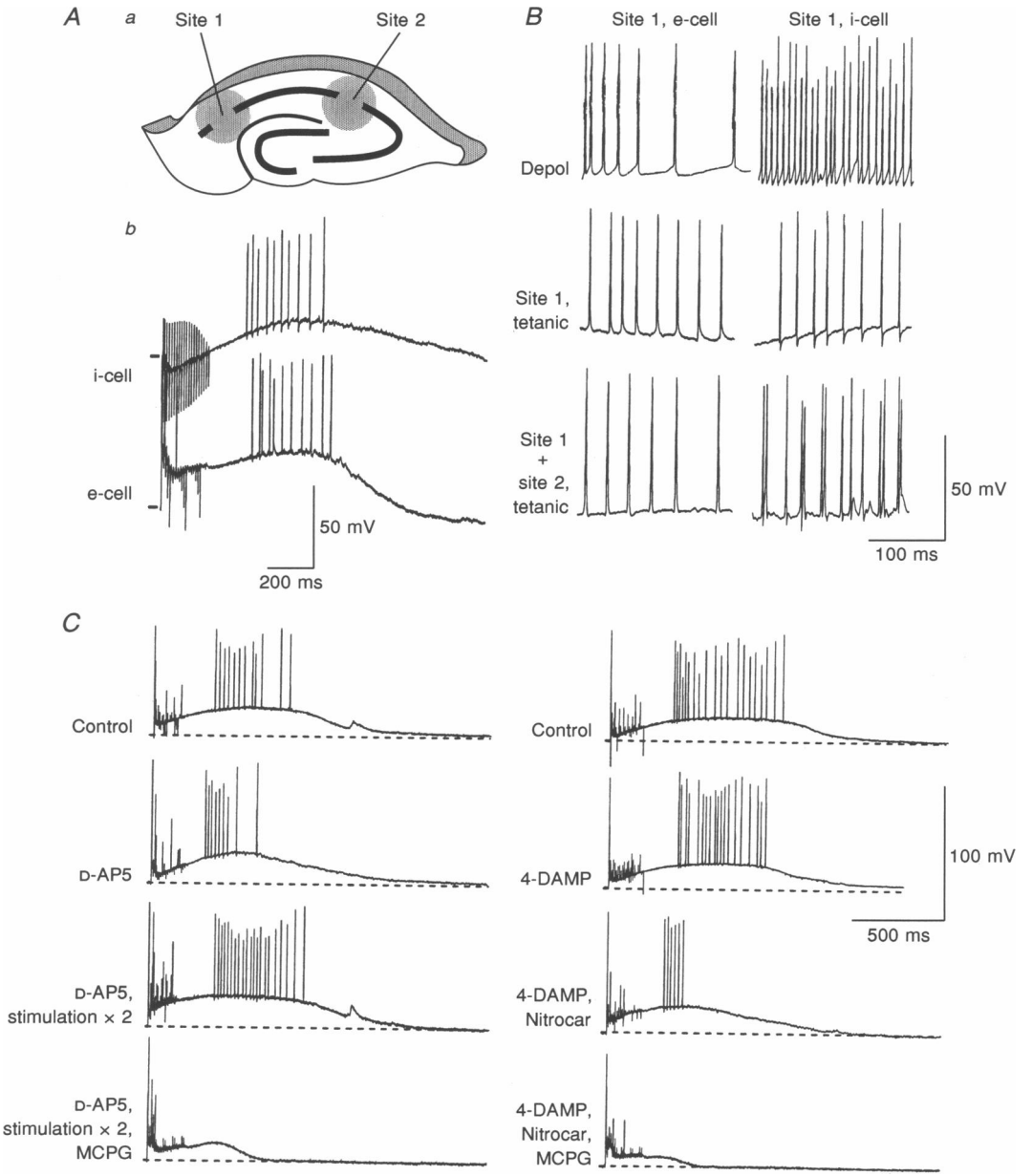

Figure 1. Intracellular correlates of tetanically evoked γ frequency oscillations

Aa, schematic diagram of transverse section of dorsal rat hippocampal slice. Tetanic stimuli were applied to the proximal dendritic region of stratum oriens at the subicular end of CA1 (Site 1), and/or to the CA2 end of CA1 (Site 2). Similar protocols were applied to longitudinal CA1 slices. Distances between sites ranged from 1·2 to 4·0 mm (transverse) and 4·5 mm (longitudinal). *Ab*, a tetanic extracellular stimulus (20 pulses at 100 Hz) produced, in both i-cells (interneurones) and e-cells (pyramidal cells), an intracellular after-depolarization followed in e-cells by an after-hyperpolarization. Rhythmic action potential generation and an underlying membrane potential oscillation were seen superimposed on the after-depolarization. This firing of action potentials is part of a population oscillation (see Fig. 4). Traces were not recorded simultaneously. *B*, e-cells responded to depolarizing current injection (Depol; 0·3 nA) with a rapidly accommodating train of action potentials (width, 4–6 ms), followed by a long after-hyperpolarization. i-cells fired a rapid train of action potentials (width, 2–3 ms; frequency about 200 Hz) with little or no accommodation and brief after-hyperpolarizations. After single-site tetanic stimulation, both e-cells and i-cells fired single action potentials at γ frequencies (40 and 46 Hz, respectively, in the example traces shown). After simultaneous two-site tetanic stimulation, e-cells fired in a similar, though slower, pattern (*ca* 30 Hz), while i-cells fired a mixture of single action potentials and action potential doublets at γ frequency. *C*, bath application of 50 μM D-AP5 reduced the duration of the post-tetanic depolarization, an effect which could be countered by increasing the stimulus strength of the tetanus (stimulation × 2). Additional application of 0·2 mM MCPG abolished the action potential oscillations and left a small, brief depolarization. The M_3 muscarinic antagonist 4-DAMP (1 μM) had no discernible effect on the oscillation or the underlying depolarization, but co-application of the M_1 muscarinic receptor antagonist Nitrocaramiphen (Nitrocar; 1 μM), reduced depolarization half-width by 50%. Additional co-application of MCPG produced complete blockade of action potential oscillations, leaving a small, brief depolarization. Dashed lines, resting potential.

Intracellular correlates of simulated network oscillation

Approximately uniform driving currents were delivered to cells in the network model, a linear chain of five groups of pyramidal cells and interneurones (see Methods). When this was done, a synchronized population oscillation was generated, as in the experimental case. As shown in Fig. 3 (top panel), pyramidal cells (e-cells) and interneurones (i-cells) both fired rhythmically at γ frequency, the interneurone usually firing spike doublets (mean within-doublet spike interval, 6 ms). Occasionally, a pyramidal cell would fire a doublet as well, but this can also happen experimentally (Fig. 1*A*). By averaging cell potentials, we confirmed that the model generated a coherent population oscillation (Fig. 3, bottom panel). The autocorrelation of the average of four e-cell potentials in group 1 was clearly rhythmic, with a frequency of 36·8 Hz. The cross-correlation between groups at opposite ends of the chain was also rhythmic, with a mean phase lag of 1·9 ms. Finally, the average relation between firing of nearby pyramidal cells and interneurones was revealed in the 'group 1 e-cell–group 1 i-cell' cross-correlation: the first spike of the interneurone doublet, on average, followed the pyramidal cell spike by only 0·6 ms. Similar behaviour was observed for three different mean driving currents.

The frequency of network oscillations increased with driving currents to the pyramidal cells. For example, when driving currents to e-cells were 1·6 nA + offsets, the frequency was 31·0 Hz; when it was 2·05 nA + offsets, the frequency was 36·8 Hz; and when it was 2·5 nA + offsets, it was 43·2 Hz.

Phase relations of pyramidal cells and interneurones

That the tetanically evoked oscillation represents a population phenomenon follows from the occurrence of population spikes (Fig. 4; see also Traub *et al.* 1996*b*). These population spikes followed the end of the tetanic stimulus with a latency of 70–190 ms for synchronous oscillations at both sites, and could reach an amplitude of 8 mV (mean, 4·8 ± 1·5 mV). This amplitude is smaller than

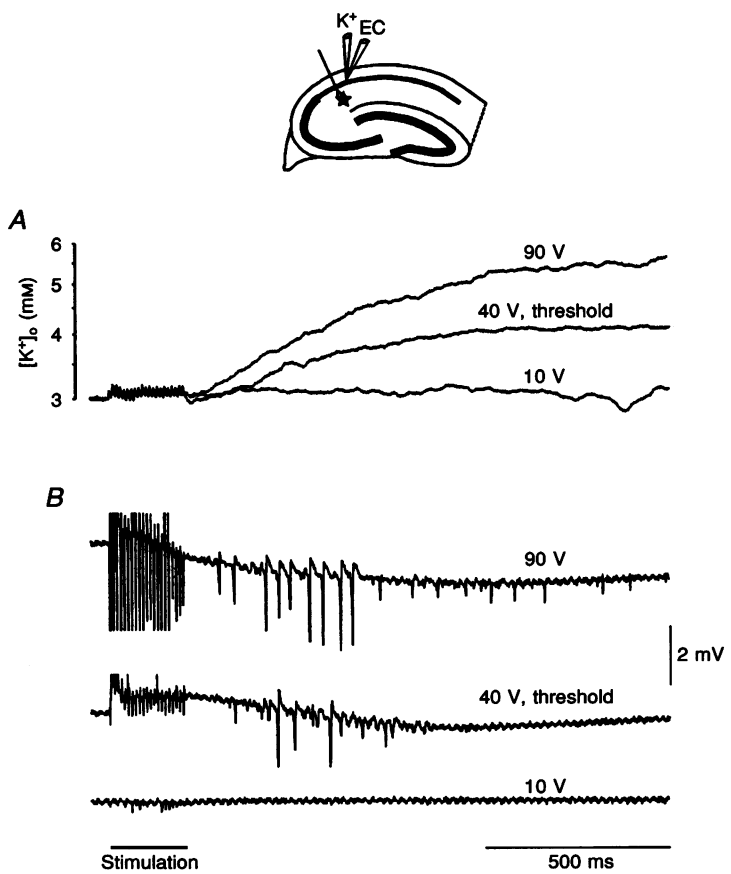

Figure 2. Measurement of γ oscillations and $[K^+]_o$

γ oscillations were evoked at the CA2 end of CA1 by tetanic stimulation (200 ms, 100 Hz, 70 V, stratum pyramidale, ★ in schematic diagram (top)). Extracellular (EC) fields and $[K^+]_o$ were measured in the CA1 pyramidal cell layer, 100 μm from the stimulating electrode. *A*, stimulus–response traces showing an increase in $[K^+]_o$ with increasing stimulation intensity. Maximal stimulation resulted in an increase in $[K^+]_o$ to about 5·5 mM. *B*, extracellular fields showing γ oscillations at 40 V stimulus strength (threshold). This γ activity corresponded to about 4·1 mM K^+_o.

the amplitude of single population spikes elicited by a single Schaffer collateral–commissural fibre volley (maximum, 12 ± 4 mV; $n = 15$ slices). With two-site stimulation, as reported previously (Traub *et al.* 1996*b*), both sites oscillate in phase (lags < 1 ms) for up to 500 ms, provided the intensity of tetanic stimulation is matched at the two sites.

The firing both of pyramidal cells and of interneurones was tightly phase-locked with nearby population spikes. The peak of pyramidal cell action potentials was within 2 ms of the peak negativity of the nearby population spike, even when there was jitter in the timing of population spikes between the two sites (Fig. 4*A*). In the case of interneurones, it was always the *first* spike of a doublet that aligned with the nearby population spike; when the interneurone fired a single action potential, this also was aligned with the nearby population spike. Using the population spike as a timing reference, we conclude that interneurones and pyramidal cells fire in phase with each other; and that when the interneurone fires a doublet, it is the first spike that is in phase with nearby pyramidal cells. This is precisely the behaviour predicted by the network model (Fig. 3; Traub *et al.* 1996*a*, *b*).

The two-site stimulation experiments revealed another interesting phenomenon. When individual population spikes at the two sites had a phase lag of a few milliseconds, interneurone doublets would 'span' the two population spikes. That is, the first action potential of the doublet was aligned with the nearby population spike, while the second action potential was aligned with the distant population spike (Fig. 4*Bd*; see also below).

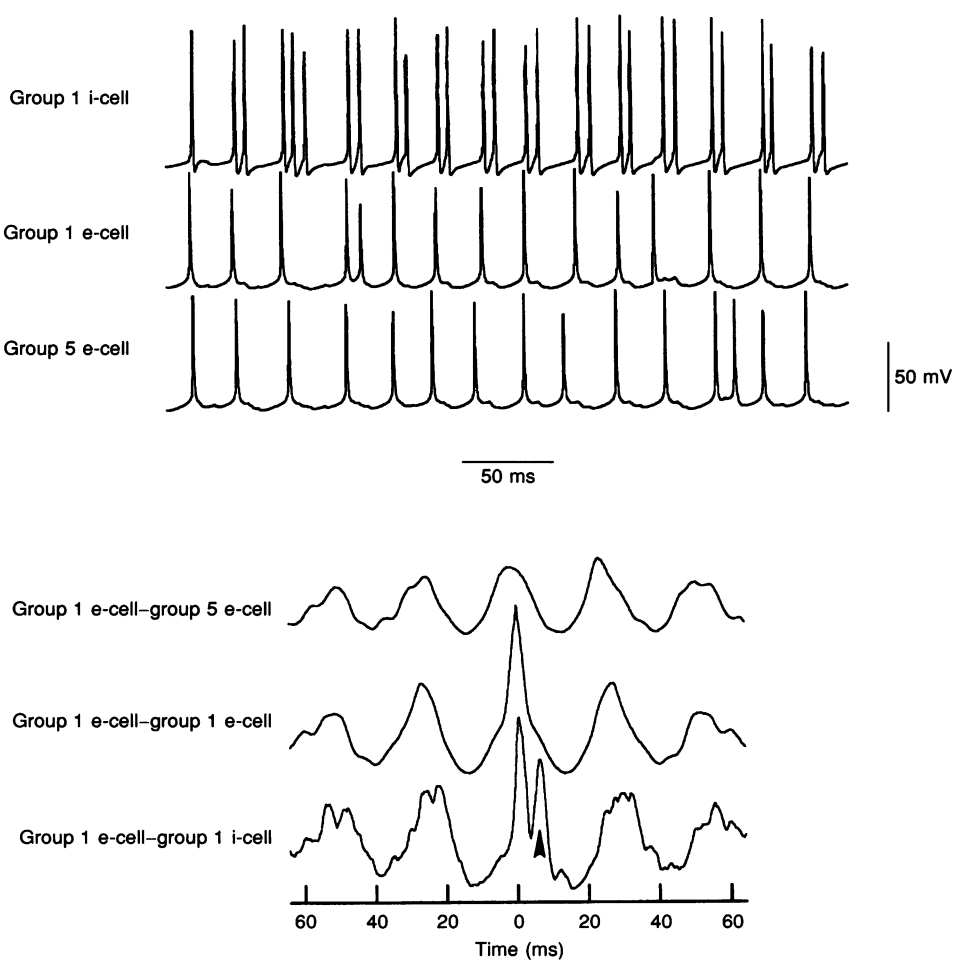

Figure 3. Summary of network model oscillatory behaviour

Tonic driving currents were applied to the e-cells (2·05 nA + small offsets, as in Methods) and to the i-cells (0·1 nA + small offsets). All of the neurones fired approximately rhythmically, the interneurones firing mostly in doublets, and the pyramidal cells mostly in singlets (top). Autocorrelations and cross-correlations (bottom) of average signals revealed that the mean population frequency was 36·8 Hz, the two ends of the network (groups 1 and 5) oscillated coherently with a mean phase lag of 1·9 ms, and the first interneurone doublet spike occurred almost simultaneously with the nearby pyramidal cell spike, on average (lag, 0·6 ms). The mean interneurone doublet interval in this case was 6·0 ms (arrowhead).

Interneurone doublet firing increases tightness of long-range synchronization, in simulations

In order to understand the contribution – in the network model – of interneurone doublets to synchronization, we manipulated the parameter $c_{e\to i}$, which scales the AMPA receptor-mediated conductance on interneurones (Fig. 5). We used a fixed set of driving currents, as well as other parameters, and repeated the simulation for a number of values of $c_{e\to i}$. For each simulation, we plotted the mean phase lag between groups 1 and 5, as well as the cross-correlation amplitude (see Methods). Oscillations were easily recognizable at single sites for all values of this parameter. In general, the phase lag was large (> 5 ms) once $c_{e\to i}$ became small enough to prevent doublet firing (*c*, Fig. 5*A* and *B*). There was, however, one value of $c_{e\to i}$, 0·16 nS, where the phase lag was 1·5 ms (data not shown). At this

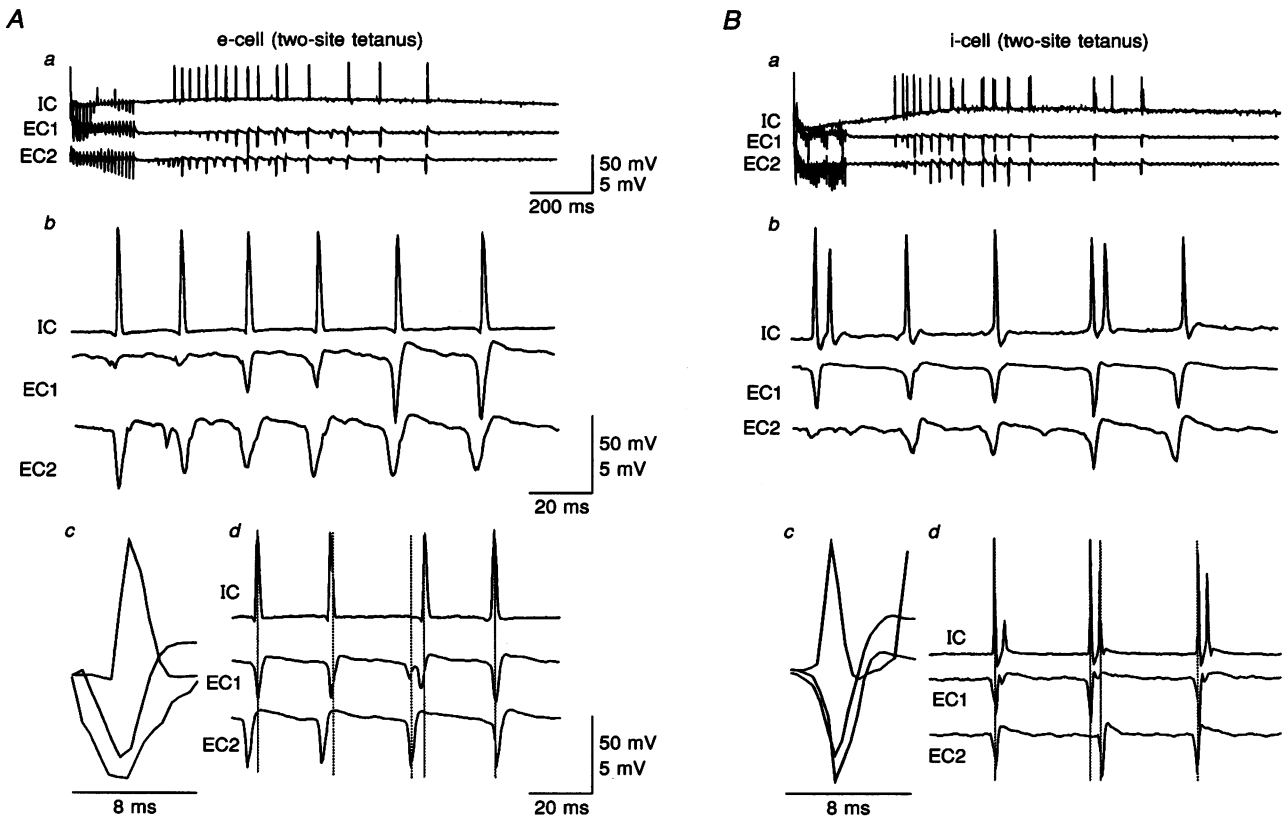

Figure 4. Characteristics of population oscillations induced in two sites in the dorsal hippocampal slice

All recordings were taken after simultaneous tetanic stimulation of sites 1 and 2, in stratum oriens. Intracellular traces were obtained from cells located at site 1, simultaneous with paired extracellular recordings. *Aa*, e-cells contribute to a population oscillation observed at both sites. Upper trace, intracellular (IC) recording of a pyramidal cell at site 1; middle trace, site 1 extracellular recording from stratum pyramidale (EC1); lower trace, extracellular recording from site 2 stratum pyramidale (EC2). Scale bar: 50 mV, IC; 5 mV, EC. *Ab*, traces of population oscillations taken 120 ms after the end of a two-site tetanic stimulation shown on an expanded time scale (traces are not those shown in *Aa*). Traces show tight synchrony of population spikes at the two sites (separation, 3 mm) and contribution to the spikes in site 1 by pyramidal cell action potentials. Scale bar: 50 mV, IC; 5 mV, EC. *Ac*, traces on a further expanded time base of simultaneous intracellular and two-site extracellular recordings showing synchrony of population spikes and action potential on a millisecond time scale. *Ad*, example of recordings showing switch from robust fixed phase lag of site 1 to millisecond scale synchronous oscillation. Scale bar: 50 mV, IC; 5 mV, EC. *Ba*, i-cells contribute to the synchronous population oscillations observed with paired tetanic stimuli. Labelling and scale bar as in *Aa*, except that the upper trace shows an IC recording of an interneurone at site 1. *Bb*, traces on an expanded time base showing i-cell doublets with the first action potential coincident with the synchronous population spikes at the two sites. Scale bar as in *Ab*. *Bc*, traces on a further expanded time base showing millisecond synchrony of population spikes and i-cell action potential. *Bd*, example traces showing phase change in population spikes accompanied by an i-cell doublet. Population spikes at site 1 occur with the first action potential of the i-cell doublets. When the two sites are out of phase (middle event), the population spike at site 2 is synchronous with the second action potential of the i-cell doublet. Scale bar as in *Ad*.

latter point, however, the cross-correlation amplitude was small. Under the conditions simulated, therefore, we may conclude that some degree of doublet firing is necessary to insure *both* a small phase lag between distant groups ($\leqslant$ 2·25 ms) and a high amplitude of the cross-correlation.

As is true in local network models (Traub, Jefferys & Whittington, 1997), loss of doublet firing is associated with an increase in frequency of the oscillation. For example, when $c_{e\rightarrow i}$ was 5·6 nS, the frequency was 31 Hz; and when $c_{e\rightarrow i}$ was zero, the frequency was 38·1 Hz. This effect occurs because the 2nd interneurone spike in the doublets acts to prolong the oscillation period. We emphasize that in this series of simulations, all other parameters – including, in particular, the driving currents to the neurones – were held constant.

Experimental blockade of AMPA receptors increases phase lags between oscillations at two sites

We were curious as to whether AMPA receptor blockade would – as predicted – lead to increases in the phase lags between the two sites. Figure 6 illustrates one experiment. When the slice was bathed in control ACSF, two-site stimulation (electrodes 1·2 mm apart) evoked oscillations with a mean frequency of 50 Hz and a mean phase lag of 1·4 ms. After addition of 20 μM NBQX to the bath, two-site

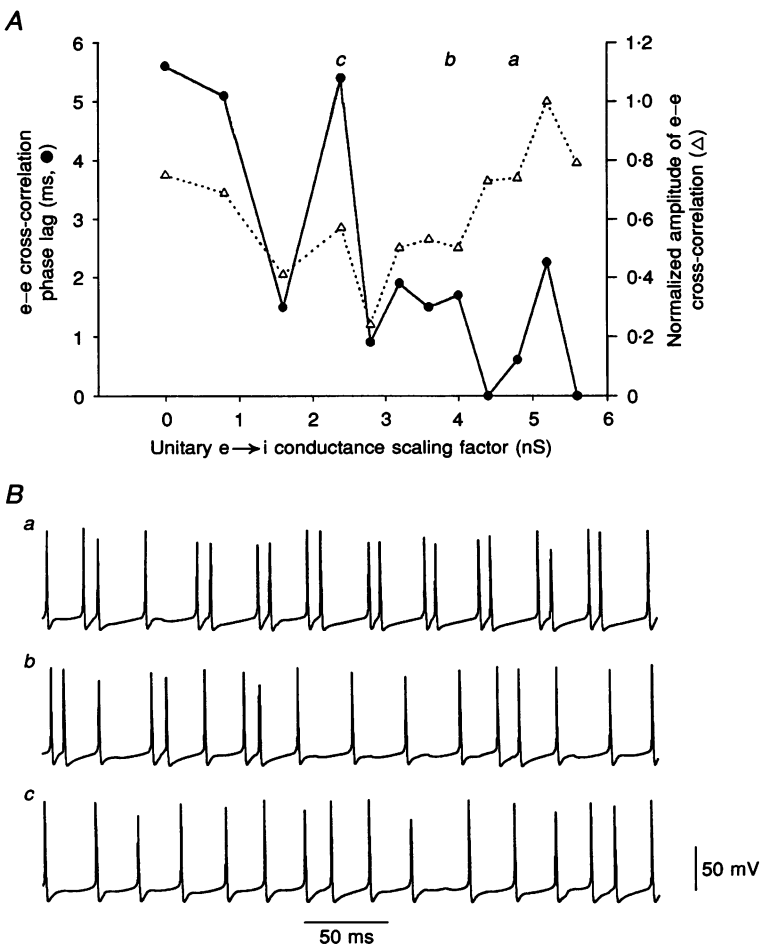

Figure 5. Effect of interneurone AMPA conductance on spatial synchronization properties: simulations

A, the network was repeatedly simulated, with e-cell driving currents of 1·6 nA + offsets, and i-cell driving currents of 0·1 nA + offsets, using different values of $c_{e\rightarrow i}$, the parameter scaling the unitary AMPA conductance at e→i connections. For each simulation, we calculated the phase lag between groups 1 and 5 (●), and the normalized amplitude of the cross-correlation between e-cells in groups 1 and 5 (△). The mean phase lag remained below 2·25 ms, once $c_{e\rightarrow i} \geqslant$ 2·8 nS. The normalized cross-correlation amplitude remained above 0·5 once $c_{e\rightarrow i} \geqslant$ 3·2 nS. When $c_{e\rightarrow i} = 0$, the phase lag was 5·6 ms. *B*, interneurone firing behaviour from three of the simulations used in *A*. *a*, doublets were usually (but not always) generated. $c_{e\rightarrow i}$, 4·8 nS; phase lag, 0·6 ms; normalized cross-correlation amplitude, 0·74. *b*, with smaller cross-correlation, doublets were intermittently present. $c_{e\rightarrow i}$, 4·0 nS; phase lag, 1·7 ms; normalized cross-correlation amplitude, 0·5. *c*, the phase lag was large and doublets were absent. $c_{e\rightarrow i}$, 2·4 nS; phase lag, 5·4 ms; normalized cross-correlation amplitude, 0·57.

simulation evoked oscillations at the same frequency, but of progressively increasing phase lag (up to 8·5 ms) as the drug washed in. Pooled data from four experiments in which the electrodes were 1·2 mm apart showed that the two sites had a phase lag of 1·85 ± 0·31 ms before and 6·70 ± 1·24 ms after addition of NBQX, just prior to the disappearance of the oscillation (20–30 min after onset of wash-in of the drug); this difference was significant ($P < 0·0002$). This increase in phase lag is as predicted by the network model (Fig. 5), by virtue of presumed blockade of AMPA receptors on interneurones.

Synchronization of the two sites is tighter at higher frequencies

How tight will synchronization between two sites be, when the stimulation to the sites is not identical? This question is of possible importance for the stability of γ frequency oscillations in the cortex *in vivo*.

In order to address this question in simulations, we made the driving currents in the network spatially non-uniform, and then examined the resulting phase lags between ends of the array. To do this, baseline currents were chosen, of

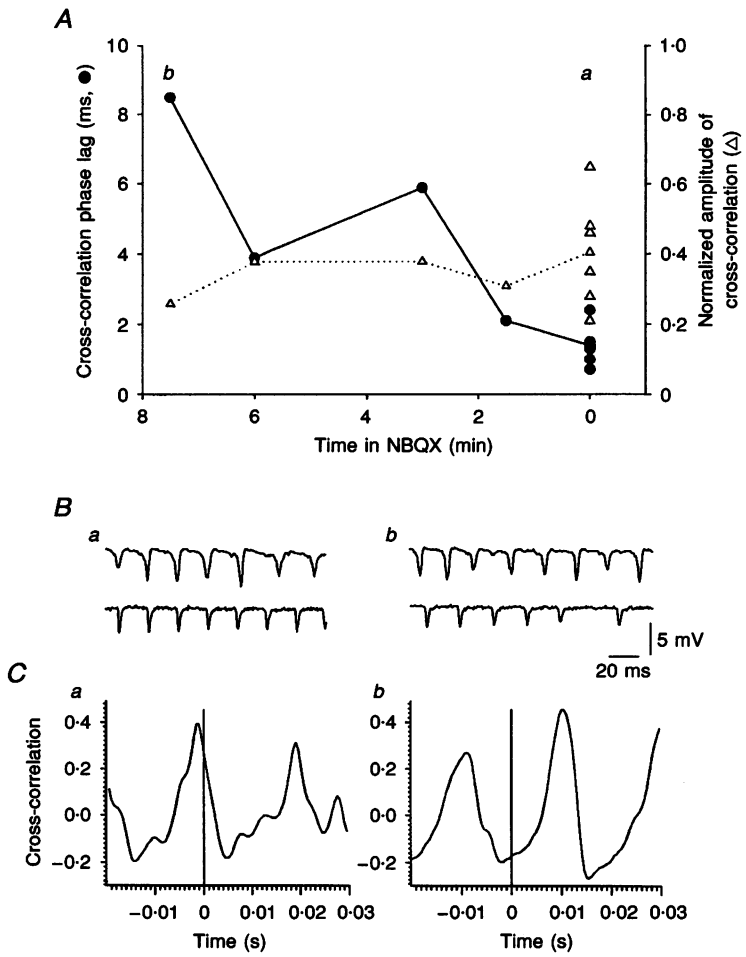

Figure 6. AMPA receptor blockade increases the phase lag between two coupled sites oscillating at γ frequency

γ frequency population oscillations were evoked by simultanous tetanic stimulation (100 Hz, 200 ms) at two sites 1·2 mm apart in the CA1 pyramidal cell layer of a transverse hippocampal slice. *A*, cross-correlations of the evoked population activity showing phase lag (●) and amplitude (△) during wash-in of NBQX (20 μM) in ACSF. Under control conditions (0 min) phase lags were < 2·3 ms (*a*). The phase lag increased with time (in minutes) after the switch to NBQX, which would lead to a gradual block of AMPA receptors. The phase lag slowed to 8·5 ms (*b*), just prior to total block of activity. The cross-correlation amplitude remained approximately constant throughout. These phase data are in agreement with simulations shown in Fig. 5. *B*, γ frequency population oscillations evoked by tetanic stimulation at the two sites 1·2 mm apart under control conditions (*a*) and just before block by NBQX (20 μM; *b*). *C*, cross-correlations of evoked actvity under control conditions (*a*) showing a phase lag of 1·4 ms and an amplitude of 0·41, and in NBQX (*b*), in which the phase lag had increased to 8·5 ms with an amplitude of 0·28. The vertical line denotes zero phase lag. Cross-correlations were determined only if the oscillation frequencies at the two sites were close; specifically, if the periods determined by autocorrelations for activity evoked at the two sites differed by no more than 1 ms, in a 150 ms time window following the inital, directly evoked, burst of coherent activity.

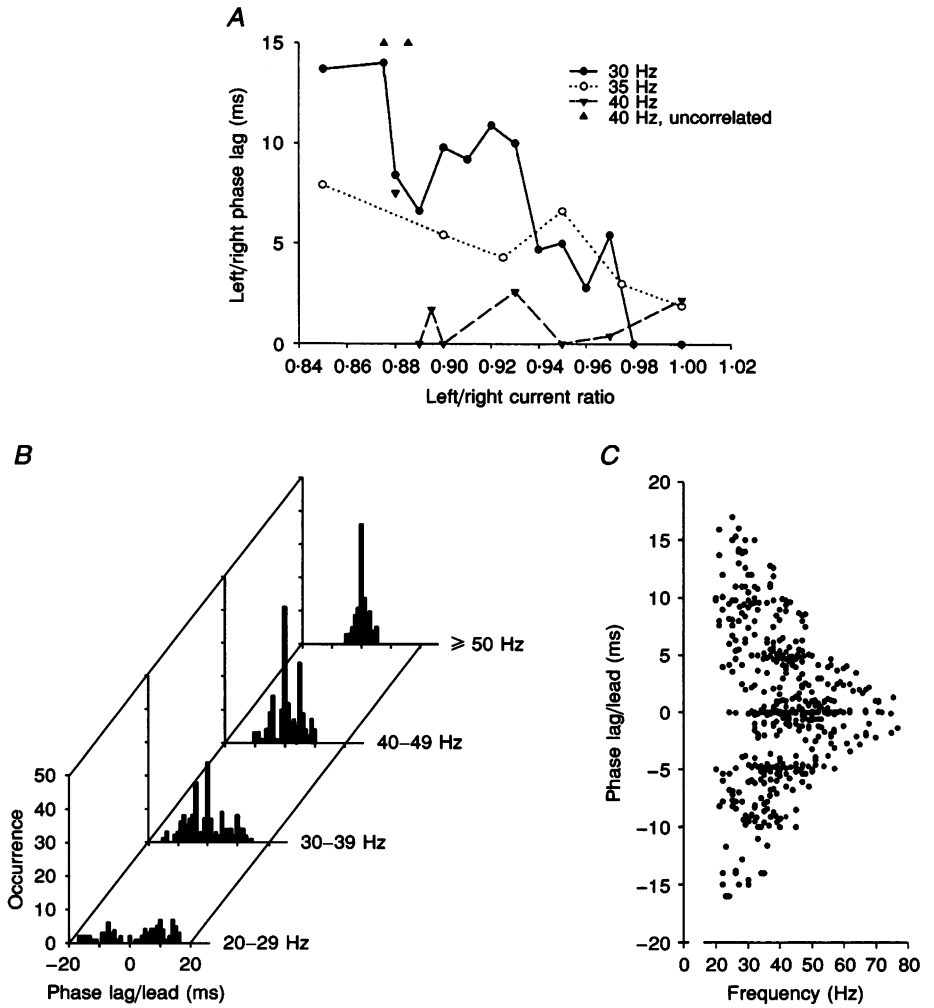

Figure 7. Occurrence of small phase intersite phase lags is most likely at higher oscillation frequencies

A, simulation data. The network was simulated with $c_{e \to i} = 8{\cdot}0$ nS, i-cell driving currents of 0·1 nA + offsets, and e-cell driving currents of either 1·6, 2·05 or 2·5 nA + offsets, both currents to cells in the right-half of the network; cells in the left-half received currents that were a fraction (left/right current ratio) of those for the right-half. This introduced spatial non-uniformity in the system, as might occur experimentally if the tetanic stimuli to the two sites were not perfectly matched. Network oscillation frequencies were clustered around 30, 35 and 40 Hz, respectively. At 40 Hz, as the current ratio decreased to 0·89, the phase lag remained below 2·6 ms; then, for small changes in current ratio, the lag fluctuated between a large value (7·5 ms) and being undefined (as the 2 sides oscillated independently). At 35 and 30 Hz, the phase lag increased (although not smoothly) as the non-uniformity increased. *B*, experimental data. Histogram of phase relationships for population spikes in oscillations evoked by two-site stratum oriens tetanic stimulation. Phase relationships were measured as the time between population spike peaks within one period at site 1 and site 2, with respect to site 1. Data were binned according to the overall train frequency as determined by cross-correlation analysis. The graph contains 532 measured phase relationships from 87 paired tetanic stimuli (the first 200 ms of the trains), from 46 slices from 25 rats. Data show little evidence for millisecond synchronization of population oscillations between the two sites at frequencies below 30 Hz. Between 30 and 49 Hz, a multimodal distribution of phase lag/lead was seen with peaks at *ca* 0 ms and ± 5 ms. As the frequency increased, the incidence of tight synchrony (zero or near-zero phase difference) also increased. *C*, scatter diagram of the phase relationships between the population spikes in sites 1 and 2 (as in *B*) plotted against the instantaneous frequency, measured as the inverse of the period immediately preceding the measured spikes. The data show that both zero and fixed phase differences can occur over a broad range of oscillation frequencies, and that as frequency increased the probability of small intersite phase differences also increased.

the form x nA + offsets to the pyramidal cells, and 0·1 nA + offsets for the interneurones; three values of x were used (1·6, 2·05 and 2·5 nA). After establishing the baseline currents, currents to the left-most twenty e-cells and i-cells were multiplied by a constant ($\leqslant 1$), the 'left/right current ratio' of Fig. 7, and the simulation was run.

These simulations showed that, at higher driving currents (i.e. oscillation frequencies), phase lags remained small ($\leqslant$ 2·6 ms) as non-uniformities developed, until the two halves of the network started to oscillate independently. At lower driving currents (frequencies), spatial uniformities led, however, to progressively longer phase lags between the two ends of the network (Fig. 7*A*).

To address experimentally the issue of spatial non-uniformity, multiple ($n = 87$) simultaneous two-site tetanic stimulations were delivered, at different absolute intensities. Data for the oscillation epochs were collected, and phase lags computed. Figure 7*B* and *C* illustrates these data in the form of a set of histograms, and as a scatter plot, respectively. In each case, it is apparent that at higher frequencies, the mean phase lag is small (S.E.M. of 1·8 ms for frequencies above 50 Hz). At lower frequencies, oscillations may occur with small phase lags as well, but also can occur with significantly longer phase lags.

Interneurone doublets decrease phase lags when driving currents are spatially non-uniform

Simulations suggest that interneurone doublets act to reduce phase lags, even when spatial inhomogeneities in stimuli prevent tight synchronization. An example of this is shown in Fig. 8. In each simulation, the baseline driving currents to e-cells were 1·6 nA + offsets, with a left/right current ratio of 0·95. In Fig. 8*A*, the parameter $c_{e\to i}$ was 8·0 nS, well over the threshold for interneurone doublets to occur (Fig. 5); in this case, the mean phase lag between groups 1 and 5 was 5·0 ms. In Fig. 8*B*, AMPA receptors on interneurones were blocked (i.e. $c_{e\to i} = 0$), preventing doublets. The phase lag in this case increased to 9 ms.

Phase relations of pyramidal cells and interneurones during non-uniform stimulation

In simulations, we examined the phase relations of interneurone doublets with average pyramidal cell potentials, under conditions in which the ends of the network were themselves out of phase with each other. An example is shown in Fig. 9. In each case, the baseline e-cell driving currents were 1·6 nA + offsets, but spatial non-uniformity was introduced in Fig. 9*B* (left/right current ratio = 0·93). In Fig. 9*A*, the mean phase lag between the ends of the network was 0·0 ms, and the first interneurone spike in the doublets lined up with the average e-cell potentials, as in

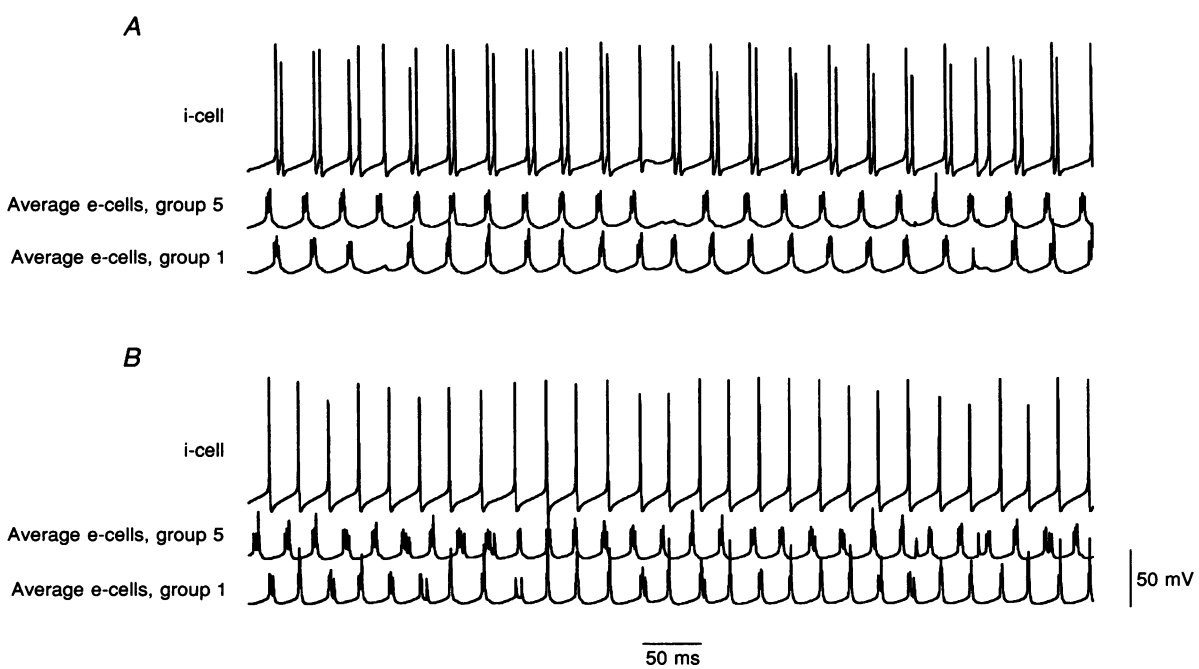

Figure 8. Interneurone spike doublets decrease phase lags when driving currents are spatially non-uniform, in simulations

Spatially non-uniform currents were used as in Fig. 7*A*, with an e-cell driving current to the right side of the network of 1·6 nA + offsets, and a current ratio of 0·95. *A*, with $c_{e\to i} = 8{\cdot}0$ nS, interneurone doublets occurred, and the mean phase lag between groups 1 and 5 was 5·0 ms. *B*, when $c_{e\to i}$ was set to 0, i.e. AMPA receptors are blocked, no interneurone doublets occurred, and the phase lag increased to 9 ms. As expected, the oscillation frequency also increased (from 29·6 to 37·8 Hz).

Figs 3 and 4*Bb*. In Fig. 9*B*, the spatial non-uniformities have introduced a mean phase lag of 10 ms between the ends of the network. Now, if an interneurone is chosen from the cell group that leads the oscillation (group 5), then the first spike of the interneurone doublet lines up with the nearby e-cells, while the second spike lines up, at least approximately, with the e-cells of the lagging cell group. This phenomenon can also be seen experimentally (Fig. 4*Bd*, central doublet).

DISCUSSION

The *in vitro* rat CA1 region is a useful model system for the study of γ frequency oscillations. It is complex enough to exhibit oscillations that are phase-locked over distances of several millimetres, with the phase depending upon a number of parameters that can be experimentally manipulated. At the same time, it appears to be simple enough to be analysed with a network simulation model that has relatively few critical structural features: three primary types of phasic synaptic interaction (pyramidal-to-interneurone, interneurone-to-pyramidal, interneurone-to-interneurone); tonic or slowly varying driving currents to pyramidal cells and interneurones; and a network structure with three spatial scales: (a) the scale of cells connecting to nearby cells with negligible axon conduction delays, (b) the next larger scale (about 0·5 mm) over which basket cell axons extend, with non-negligible axon conduction delays, and (c) the still larger scale over which synchronized oscillations can occur (4·5 mm at least).

The network model makes three important predictions that appear to be confirmed by previously reported data and data in this study.

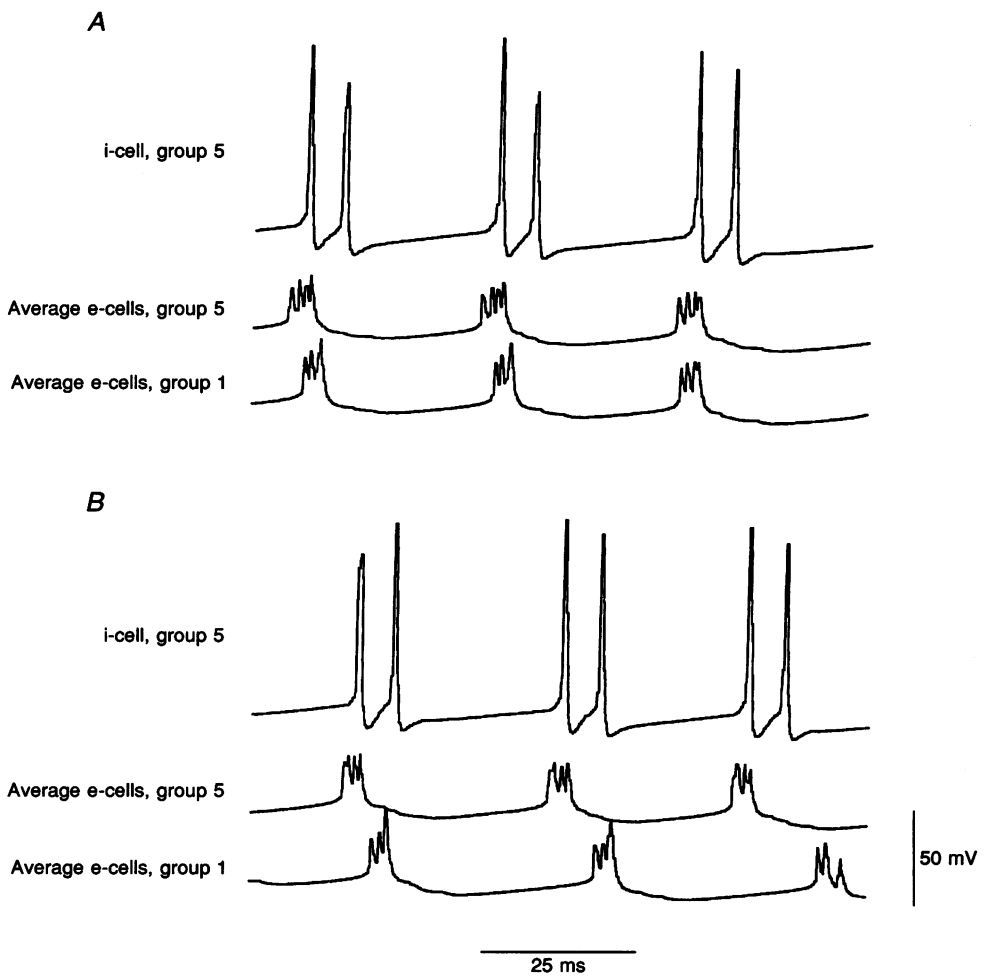

Figure 9. Interneurone doublets in the model can 'line up' with e-cell firings at both ends of the network

Simulations were done with driving currents to the right side of the network of 1·6 nA + offsets for e-cells, and 0·1 nA + offsets for i-cells. The left/right current ratio was 1·0 for *A* and 0·93 for *B* (see legend to Fig. 7). *A*, mean phase lag between groups 1 and 5 was 0 ms. The first spike of interneurone doublets is aligned with the average e-cell potentials (see also Fig. 3). *B*, there was now a mean phase lag of 10 ms between groups 1 and 5. The first spike of the interneurone doublet is aligned with the local e-cells, while the second spike is approximately aligned with the distant (lagging) e-cells. Compare with Fig. 4.

Prediction 1

The frequency of γ oscillations is lower in large oscillating ensembles than in small ensembles (Traub *et al.* 1996*b*). This is physically reasonable because the coupling between neighbouring cell groups is either directly inhibitory, or takes place via excitation of inhibitory neurones; hence, each cell group will tend to delay the firing of connected cell groups. In particular, doublet or multiplet firing by interneurones, which is most likely to occur when cell groups are coupled, will tend to slow the oscillation by generating polyphasic IPSPs in e-cells and i-cells (Traub *et al.* 1997).

Prediction 2

Interneurone doublet firing is most likely to occur when long-range synchrony exists (Traub *et al.* 1996*b*). This is attributable to the increased synaptic excitation of interneurones that will occur when the population of synchronously firing pyramidal cells increases. In simulations, even locally synchronized populations of pyramidal cells would be expected to induce doublet firing in interneurones, provided the e→i synapse has a large enough conductance (Traub *et al.* 1997). Experimentally, however, we have never observed interneurone doublets after single-site stimulation.

In many simulations, doublets occur in each interneurone, and on most of the γ waves, whereas, in the experiments, some interneurones (2/8) do not fire doublets, and others fire doublets, but not on each γ wave. In the latter case, however, a post-spike depolarization is often seen, which probably represents summated EPSPs that are subthreshold for firing the cell. It is possible that the e→i AMPA conductance in the model is too large. Other factors that should be considered include: (a) synaptic failures are not simulated; (b) there are sampling problems with the interneurone recordings, in that not all interneurones necessarily participate in the oscillation identically; and (c) driving currents to the interneurones may be time dependent, unlike the time-independent currents used in the model.

In any case, the model can still produce long-range synchrony in cases when doublet firing is not continuous, at the cost of some decrease in the cross-correlation amplitude (Fig. 5).

Prediction 3

Pyramidal cells fire in phase with the first spike in doublets from nearby interneurones (Figs 3, 4 and 9; Traub *et al.* 1996*b*). This is a consequence of the fact that the pyramidal cells and the interneurones 'experience' IPSPs generated by the same presynaptic interneurones (in the case of the interneurones, it is just the interneurones themselves). In the model, this tight phase relation occurs over a range of driving currents to the interneurones, but not for all driving currents; if the latter are too small or too large, phase lags (or leads, respectively) occur in the interneurones relative to the pyramidal cells. Phase lags were noted only when the interneurones were hyperpolarized (not shown), which does not occur during experimental oscillations in our hands. Excessive synaptic drives perhaps do not occur experimentally because of the finite number of glutamate receptors (particularly metabotropic glutamate receptors) on the interneurones; this is consistent with our inability to produce interneurone network γ at frequencies above about 50 Hz, by activation of metabotropic glutamate receptors (Traub *et al.* 1996*a*).

Our results suggest two new conclusions.

Conclusion 1

The firing of spike doublets by interneurones appears to be causally related to the generation of γ oscillations synchronized tightly over several millimetres, rather than just an epiphenomenon of the circuit connections. There are two pieces of experimental evidence that support this conclusion. First, as predicted (Fig. 5; Traub *et al.* 1996*b*), pharmacological blockade of AMPA receptors – which is expected to prevent interneurone doublets from occurring – disrupts the ability of the CA1 region to produce γ oscillations that are synchronized over more than 1 mm, with phase lags < 2 ms (Fig. 6). Second, the model correctly predicts the frequency dependence of stable phase lags during γ oscillations, these lags being more likely at lower frequencies than at higher frequencies, and, as predicted, the lags are associated with interneurone doublets that are aligned with population spikes at either end of the array (Figs 4 and 9). We are not yet in a position to analyse quantitatively how many doublets are necessary for synchronization. First, the model contains too few cells and has an idealized network connectivity. Second, we do not know how often – when interneurones fire single spikes followed by a large EPSP – spike doublets occur in the axon (i.e. we do not know the true frequency of doublets in the network). Non-synaptic mechanisms are unlikely to provide long-range synchronization on a 1 ms time scale. Haas & Jefferys (1984) recorded a maximum conduction velocity of 0·12 m s^{-1} for population spikes in low-calcium CA1 field bursts; this corresponds to a delay of 17 ms over 2 mm.

A critical role of interneurone doublets would have one further implication: γ oscillations *in vivo* that are synchronized over many millimetres with short phase lags may not represent 'interneurone network γ', as studied previously (Traub *et al.* 1996*a*), but may rather represent a phenomenon built 'on top of' interneurone network γ, a co-operative phenomenon between pyramidal cells and interneurones, with both playing an essential part.

Conclusion 2

Widespread synchrony of γ oscillations *in vivo* could, in principle, arise solely via intracortical mechanisms. Longitudinal hippocampal slices can exhibit γ oscillations that are synchronized tightly over 4·5 mm at least, a distance approaching the 7 mm reported for tight synchronization of

γ oscillations in the visual cortex *in vivo* (Gray *et al.* 1989). This is not to say that *in vivo* γ oscillations actually do arise purely intracortically. One study has reported that γ oscillations might arise within the cortex, at least sometimes (Barth & MacDonald, 1996). On the other hand, a number of studies have demonstrated γ oscillations that are tightly phase-locked between thalamus and cortex (Steriade *et al.* 1996*a*; Steriade, Contreras, Amzica & Timofeev, 1996*b*), as well as γ oscillations (at rather high frequencies) in the thalamus that are driven by the retina (Neuenschwander & Singer, 1996). Furthermore, magnetic recordings in humans suggest that γ oscillations are thalamocortical (Ribary *et al.* 1991). While our data are useful in understanding the cortical circuitry that might contribute to the generation of γ oscillations *in vivo*, it is premature to draw conclusions about the entire thalamocortical system.

AMPA receptors on interneurones

Given that the e→i synaptic connection appears to be critical for long-range tight synchrony of γ oscillations, and given that such synchrony is probably of importance for brain function, the molecular and electrophysiological properties of these AMPA receptors assume particular importance. AMPA receptors on at least certain interneurones have distinct functional properties *vis-à-vis* AMPA receptors on pyramidal cells: the unitary EPSC is of abrupt onset, large amplitude, and decays quickly (Miles, 1990), and interneurone AMPA receptor channels are relatively permeable to calcium and rectify at strongly depolarized membrane potentials (Iino, Ozawa & Tsuzuki, 1990). These properties depend on receptor subunit composition (particularly the relative absence of GluR-B in interneurones and perhaps on the relative presence of GluR-D) and are regulated by post-translational alternative splicing and RNA editing (Bochet *et al.* 1994; Geiger *et al.* 1995). We suggest that the functional reliability of the e→i connection (which can even allow unitary EPSPs to elicit action potentials (Knowles & Schwartzkroin, 1981; Lacaille *et al.* 1987; Miles, 1990)) takes on biological meaning because of the role interneurones play in high-frequency cortical oscillations, with the apparent necessity for interneurone doublets to occur during long-range synchrony of firing, and that use-dependent increases in efficacy of excitatory synapses on interneurones (Taube & Schwartzkroin, 1987; Ouardouz & Lacaille, 1995) may be important for the same reason.

Barth, D. S. & MacDonald, K. D. (1996). Thalamic modulation of high-frequency oscillating potentials in auditory cortex. *Nature* **383**, 78–81.

Bochet, P., Audinat, E., Lambolez, B., Crépel, F., Rossier, J., Iino, M., Tsuzuki, K. & Ozawa, S. (1994). Subunit composition at the single-cell level explains functional properties of a glutamate-gated channel. *Neuron* **12**, 383–388.

Borroni, A. M. & Levy, W. B. (1996). Gamma oscillations in CA1 mini-slices. *Society for Neuroscience Abstracts* **22**, 670.

Bragin, A., Jandó, G., Nádasdy, Z., Hetke, J., Wise, K. & Buzsáki, G. (1995). Gamma (40–100 Hz) oscillation in the hippocampus of the behaving rat. *Journal of Neuroscience* **15**, 47–60.

Buhl, E. H., Cobb, S. R., Halasy, K. & Somogyi, P. (1995). Properties of unitary IPSPs evoked by anatomically identified basket cells in the rat hippocampus. *European Journal of Neuroscience* **7**, 1989–2004.

Buhl, E. H., Han, Z.-S., Lörinczi, Z., Stezhka, V. V., Karnup, S. V. & Somogyi, P. (1994). Physiological properties of anatomically identified axo-axonic cells in the rat hippocampus. *Journal of Neurophysiology* **71**, 1289–1307.

Christian, E. P. & Dudek, F. E. (1988). Electrophysiological evidence from glutamate microapplications for local excitatory circuits in the CA1 area of rat hippocampal slices. *Journal of Neurophysiology* **59**, 110–123.

Engel, A. K., Kreiter, A. K., König, P. & Singer, W. (1991). Synchronization of oscillatory neuronal responses between striate and extrastriate visual cortical areas of the cat. *Proceedings of the National Academy of Sciences of the USA* **88**, 6048–6052.

Frien, A., Eckhorn, R., Bauer, R., Woelbern, T. & Kehr, H. (1994). Stimulus-specific fast oscillations at zero phase between visual areas V1 and V2 of awake monkey. *NeuroReport* **5**, 2273–2277.

Geiger, J. R. P., Melcher, T., Koh, D.-S., Sakmann, B., Seeburg, P. H., Jonas, P. & Monyer, H. (1995). Relative abundance of subunit mRNAs determines gating and Ca^{2+} permeability of AMPA receptors in principal neurons and interneurons in rat CNS. *Neuron* **15**, 193–204.

Gray, C. M., König, P., Engel, A. K. & Singer, W. (1989). Oscillatory responses in cat visual cortex exhibit inter-columnar synchronization which reflects global stimulus properties. *Nature* **338**, 334–337.

Haas, H. L. & Jefferys, J. G. R. (1984). Low-calcium field burst discharges of CA1 pyramidal neurones in rat hippocampal slices. *Journal of Physiology* **354**, 185–201.

Heinemann, U., Lux, H. D. & Gutnick, M. J. (1977). Extracellular free calcium and potassium during paroxysmal activity in the cerebral cortex of the cat. *Experimental Brain Research* **27**, 237–243.

Iino, M., Ozawa, S. & Tsuzuki, K. (1990). Permeation of calcium through excitatory amino acid receptor channels in cultured rat hippocampal neurones. *Journal of Physiology* **424**, 151–165.

Knowles, W. D. & Schwartzkroin, P. A. (1981). Local circuit synaptic interactions in hippocampal brain slices. *Journal of Neuroscience* **1**, 318–322.

König, P., Engel, A. K., Roelfsema, P. R. & Singer, W. (1995). How precise is neuronal synchronization? *Neural Computation* **7**, 469–485.

Lacaille, J.-C., Mueller, A. L., Kunkel, D. D. & Schwartzkroin, P. A. (1987). Local circuit interactions between oriens/alveus interneurons and CA1 pyramidal cells in hippocampal slices: electrophysiology and morphology. *Journal of Neuroscience* **7**, 1979–1993.

Miles, R. (1990). Synaptic excitation of inhibitory cells by single CA3 hippocampal pyramidal cells of the guinea-pig *in vitro*. *Journal of Physiology* **428**, 61–77.

Murakoshi, T., Guo, J.-Z. & Ichinose, T. (1993). Electrophysiological identification of horizontal synaptic connections in rat visual cortex *in vitro*. *Neuroscience Letters* **163**, 211–214.

MURTHY, V. N. & FETZ, E. E. (1992). Coherent 25- to 35-Hz oscillations in the sensorimotor cortex of awake behaving monkeys. *Proceedings of the National Academy of Sciences of the USA* **89**, 5670–5674.

NEUENSCHWANDER, S. & SINGER, W. (1996). Long-range synchronization of oscillatory light responses in the cat retina and lateral geniculate nucleus. *Nature* **379**, 728–733.

OUARDOUZ, M. & LACAILLE, J.-C. (1995). Mechanisms of selective long-term potentiation of excitatory synapses in stratum oriens/alveus interneurons of rat hippocampal slices. *Journal of Neurophysiology* **73**, 810–819.

POZZO MILLER, L. D., PETROZZINO, J. J. & CONNOR, J. A. (1995). G protein-coupled receptors mediate a fast excitatory postsynaptic current in CA3 pyramidal neurons in hippocampal slices. *Journal of Neuroscience* **15**, 8320–8330.

RIBARY, U., IOANNIDES, A. A., SINGH, K. D., HASSON, R., BOLTON, J. P. R., LADO, F., MOGILNER, A. & LLINÁS, R. (1991). Magnetic field tomography of coherent thalamocortical 40-Hz oscillations in humans. *Proceedings of the National Academy of Sciences of the USA* **88**, 11037–11041.

SALIN, P. A. & PRINCE, D. A. (1996). Electrophysiological mapping of $GABA_A$ receptor-mediated inhibition in adult rat somatosensory cortex. *Journal of Neurophysiology* **75**, 1589–1600.

SCHWARTZKROIN, P. A. (1978). Secondary range rhythmic spiking in hippocampal neurons. *Brain Research* **149**, 247–250.

SIK, A., PENTTONEN, M., YLINEN, A. & BUZSÁKI, G. (1995). Hippocampal CA1 interneurons: an *in vivo* intracellular labeling study. *Journal of Neuroscience* **115**, 6651–6665.

SINGER, W. & GRAY, C. M. (1995). Visual feature integration and the temporal correlation hypothesis. *Annual Review of Neuroscience* **18**, 555–586.

STERIADE, M., AMZICA, F. & CONTRERAS, D. (1996*a*). Synchronization of fast (30–40 Hz) spontaneous cortical rhythms during brain activation. *Journal of Neuroscience* **16**, 392–417.

STERIADE, M., CONTRERAS, D., AMZICA, F. & TIMOFEEV, I. (1996*b*). Synchronization of fast (30–40 Hz) spontaneous oscillations in intrathalamic and thalamocortical networks. *Journal of Neuroscience* **16**, 2788–2808.

TAMAMAKI, N. & NOJYO, Y. (1990). Disposition of the slab-like modules formed by axon branches originating from single CA1 pyramidal neurons in the rat hippocampus. *Journal of Comparative Neurology* **291**, 509–519.

TAUBE, J. S. & SCHWARTZKROIN, P. A. (1987). Intracellular recording from hippocampal CA1 interneurons before and after development of long-term potentiation. *Brain Research* **419**, 32–38.

THOMSON, A. M. & RADPOUR, S. (1991). Excitatory connection between CA1 pyramidal cells revealed by spike triggered averaging in slices of rat hippocampus are partially NMDA receptor mediated. *European Journal of Neuroscience* **3**, 587–601.

TRAUB, R. D., JEFFERYS, J. G. R., MILES, R., WHITTINGTON, M. A. & TÓTH, K. (1994). A branching dendritic model of a rodent CA3 pyramidal neurone. *Journal of Physiology* **481**, 79–95.

TRAUB, R. D., JEFFERYS, J. G. R. & WHITTINGTON, M. A. (1997). Simulation of gamma rhythms in networks of interneurons and pyramidal cells. *Journal of Computational Neuroscience* **4**, 141–150.

TRAUB, R. D. & MILES, R. (1995). Pyramidal cell-to-inhibitory cell spike transduction explicable by active dendritic conductances in inhibitory cell. *Journal of Computational Neuroscience* **2**, 291–298.

TRAUB, R. D., WHITTINGTON, M. A., COLLING, S. B., BUZSÁKI, G. & JEFFERYS, J. G. R. (1996*a*). Analysis of gamma rhythms in the rat hippocampus *in vitro* and *in vivo*. *Journal of Physiology* **493**, 471–484.

TRAUB, R. D., WHITTINGTON, M. A., STANFORD, I. M. & JEFFERYS, J. G. R. (1996*b*). A mechanism for generation of long-range synchronous fast oscillations in the cortex. *Nature* **383**, 621–624.

WHITTINGTON, M. A., TRAUB, R. D. & JEFFERYS, J. G. R. (1995). Synchronized oscillations in interneuron networks driven by metabotropic glutamate receptor activation. *Nature* **373**, 612–615.

WONG, R. K. S. & PRINCE, D. A. (1981). Afterpotential generation in hippocampal pyramidal cells. *Journal of Neurophysiology* **45**, 86–97.

Acknowledgements

This work was supported by The Wellcome Trust and the Human Frontier Science Program (slice experiments) and by IBM (computer simulations). We thank Drs Hannah Monyer and György Buzsáki for helpful discussions. R.D.T. is a Wellcome Principal Research Fellow.

Author's email address

R. D. Traub: r.d.traub@bham.ac.uk

Received 3 December 1996; accepted 24 April 1997.